# Planar Bipedal Locomotion with Nonlinear Model Predictive Control: Online Gait Generation using Whole-Body Dynamics

Manuel Y. Galliker[1†], Noel Csomay-Shanklin[2†], Ruben Grandia[1], Andrew J. Taylor[2], Farbod Farshidian[1], Marco Hutter[1], Aaron D. Ames[2]

***Abstract*— The ability to generate dynamic walking in real-time for bipedal robots with input constraints and underactuation has the potential to enable locomotion in dynamic, complex and unstructured environments. Yet, the high-dimensional nature of bipedal robots has limited the use of full-order rigid body dynamics to gaits which are synthesized offline and then tracked online. In this work we develop an online nonlinear model predictive control approach that leverages the full-order dynamics to realize diverse walking behaviors. Additionally, this approach can be coupled with gaits synthesized offline via a desired reference to enable a shorter prediction horizon and rapid online re-planning, bridging the gap between online reactive control and offline gait planning. We demonstrate the proposed method, both with and without an offline gait, on the planar robot AMBER-3M in simulation and on hardware.**

## I. Introduction

In order for bipedal robots to reach their full potential of navigating complex terrain inaccessible by wheeled robots, it is necessary for them to demonstrate a rich set of dynamically stable locomotion behaviors. Achieving this, especially while leveraging phases of underactuation like their human counterparts do, necessitates the dynamic coordination of the whole-body dynamics of the robot. Planning for the next foot strike must occur throughout the step in a manner that accounts for the inherently nonlinear passive dynamics of the system. Achieving diverse locomotion behaviors in complex environments, therefore, motivates that whole-body planning be done on the robot in real-time, thereby going beyond pre-planned periodic walking gaits.

Many approaches for achieving locomotion use condensed stability conditions like Zero-Moment Point (ZMP) [1], or rely on other reduced-order models that simplify elements such as leg mass [2], [3]. In contrast, Model Predictive Control (MPC) provides a tool for the online synthesis of general, *aperiodic trajectories*, allowing feedback of environmental parameters to be incorporated into dynamic motion planning [4], [5]. In particular, by optimizing directly

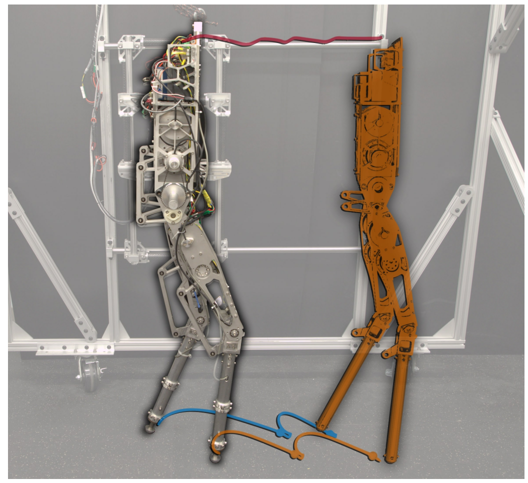

Fig. 1: AMBER-3M platform using the whole-body nonlinear MPC incorporating an HZD gait. The optimized feet and torso trajectories are visualized along the prediction horizon.

over contact forces, these methods have seen significant use in online motion planning for quadrupedal robotics, with extensive experimental results [6]. Whole-body motion planning results for bipedal walking have been predominantly in simulation [7], [8] or used whole-body planning only for non-walking tasks such as reaching [9]. Notably, the online motion planning tools with remarkable experimental results for quadrupedal locomotion have not yet achieved commensurate results for bipedal robotics.

One of the key challenges in online whole-body motion planning is computational limitations, as producing stable locomotion requires optimizing over a sufficiently long horizon. The methods for quadrupeds that have yielded experimental results typically exploit low leg inertia to neglect leg dynamics, reducing the state dimension in the optimization. Transferring this reduction to bipedal systems is difficult, however, as the legs compose a relatively high fraction of the system's total inertia. At the same time, simultaneously considering both leg and torso dynamics results in many degrees of freedom, making optimization over long time horizons computationally intensive. Furthermore, the narrow stance width and high center of mass of bipeds necessitate a high planning frequency to counteract disturbances in underactuated dimensions. Thus, it is paramount to design whole-body motion planners that balance the trade-off between horizon length, model complexity, and planning frequency.

We make three contributions in this work. First, we propose a nonlinear MPC approach for online whole-body

† These authors contributed equally to this work.

[1] M. Y. Galliker, R. Grandia, F. Farshidian, and M. Hutter are with the Department of Mechanical and Process Engineering, ETH Zürich, 8092 Zürich, Switzerland {manuelga, rgrandia, farbodf, mahutter}@ethz.ch

[2] N. Csomay-Shanklin, A. J. Taylor, and A. D. Ames are with the Department of Computing and Mathematical Sciences, California Institute of Technology, Pasadena, CA, 91125, USA {noelcs, ajtaylor, ames}@caltech.edu

This research was supported by NSF NRI award 1924526, NSF award 1932091, NSF CMMI award 1923239, and the Swiss National Science Foundation through the National Centre of Competence in Research Robotics (NCCR Robotics).

motion planning of bipedal robotic locomotion based on existing methods used for quadrupedal locomotion [10], which achieved a wide range of stable behaviors with a planning horizon of 2 s and update frequency of up to 270 Hz. Second, to reduce the computational burden of online whole-body planning, we incorporate a stable periodic walking gait synthesized offline via Hybrid Zero Dynamics (HZD) [11] into the nonlinear optimization problem. This information permits robust walking while optimizing over shorter horizon lengths (0.2 s) that require less computational effort and allow rapid re-planning (850 Hz) – this will be important for achieving whole-body planning on 3D walking systems. Lastly, we experimentally validate the proposed approach on the planar bipedal robot AMBER-3M [12], demonstrating standing, stepping in place, and walking. To the best of our knowledge, this is the first experimental demonstration of online whole-body locomotion planning for bipedal walking.

## II. Whole-Body Motion Planning & Control

Nonlinear MPC solves a optimization problem in a receding horizon manner by solving the following finite time nonlinear optimal control problem:

$$\begin{aligned}
\underset{\mathbf{u}(\cdot)}{\text{minimize}} \quad & \phi(\mathbf{x}(t_H)) + \int_0^{t_H} l(\mathbf{x}(t), \mathbf{u}(t), t)\mathrm{d}t, && \text{(1a)}\\
\text{subject to:} \quad & \mathbf{x}(0) = \mathbf{x}_0, && \text{(1b)}\\
& \dot{\mathbf{x}} = \mathbf{f}(\mathbf{x}) + \mathbf{g}(\mathbf{x})\mathbf{u}, && \text{(1c)}\\
& \mathbf{x}(t_i^+) = \Delta_c(\mathbf{x}(t_i)), && \text{(1d)}\\
& \mathbf{h}_{eq}(\mathbf{x}, \mathbf{u}, t) = \mathbf{0}, && \text{(1e)}\\
& \mathbf{h}_{in}(\mathbf{x}, \mathbf{u}, t) \geq \mathbf{0}, && \text{(1f)}
\end{aligned}$$

where $t_H$ is the length of the horizon, $\phi : \mathcal{X} \to \mathbb{R}$ is the terminal cost, $l : \mathcal{X} \times \mathbb{R}^m \times \mathbb{R} \to \mathbb{R}$ is the time-varying running state-input cost, and $t_i$ are times of contact mode transitions. The optimal control problem is solved in real-time by updating the initial conditions (1b) with the measured state of the system. Eq. (1c) describes the system dynamics. $\mathbf{h}_{eq} : \mathcal{X} \times \mathbb{R}^m \times \mathbb{R} \to \mathbb{R}^{eq}$ and $\mathbf{h}_{in} : \mathcal{X} \times \mathbb{R}^m \times \mathbb{R} \to \mathbb{R}^{in}$ are generalized path equality and inequality constraints, respectively. To solve this problem we take a direct-multiple shooting transcription of the problem together with a sequential quadratic programming approach to handle nonlinearities [13]

Our nonlinear MPC problem will be constructed using the *OCS2* toolbox [14], which provides convenient interfaces to the *Pinocchio* [15] rigid body library and *CppAd* [16] automatic differentiation tools. Our formulation assumes that the contact schedule associated with a given locomotion mode (standing, stepping in place, walking) is given by the user. The fixed contact schedule assumption simplifies the optimization problem as the sequence of domains and timing of contact mode transitions does not need to be optimized [4], [10]. The position of the foot at contact is captured in the optimization problem through its kinematic relationship with joint coordinates. Moreover, we assume the user provides a desired base pose and velocity to the MPC.

### A. System Dynamics

The configuration of the robot may be described by a set of $d$ generalized coordinates:

$$\mathbf{q} = \begin{bmatrix}\mathbf{q}_b^\top & \mathbf{q}_j^\top\end{bmatrix}^\top \in \mathcal{Q} \triangleq SE(3) \times \mathcal{Q}_j, \tag{2}$$

which include the base coordinates $\mathbf{q}_b$ and joint coordinates $\mathbf{q}_j$ of the robot, respectively. The joint coordinates are assumed to be fully actuated.

Using the Euler-Lagrange method, the system dynamics corresponding to base and joint components in a contact domain $\mathcal{D}_c$ are given by:

$$\begin{bmatrix}\mathbf{D}_{bb}, & \mathbf{D}_{bj}\\ \mathbf{D}_{bj}^\top & \mathbf{D}_{jj}\end{bmatrix}\begin{bmatrix}\ddot{\mathbf{q}}_b\\ \ddot{\mathbf{q}}_j\end{bmatrix} + \begin{bmatrix}\mathbf{h}_b\\ \mathbf{h}_j\end{bmatrix} = \begin{bmatrix}\mathbf{0}\\ \mathbf{B}_j\end{bmatrix}\boldsymbol{\tau} + \begin{bmatrix}\mathbf{J}_{c,b}^\top\\ \mathbf{J}_{c,j}^\top\end{bmatrix}\boldsymbol{\lambda}. \tag{3}$$

with symmetric positive definite inertia matrix $\mathbf{D} : \mathcal{Q} \to \mathbb{S}^d_{\succ 0}$, centrifugal, Coriolis, and gravitational terms $\mathbf{h} : \mathcal{X} \to \mathbb{R}^d$, actuation matrix $\mathbf{B} : \mathcal{Q} \to \mathbb{R}^{d\times m}$, torques $\boldsymbol{\tau} \in \mathbb{R}^m$, constraint forces $\boldsymbol{\lambda} \in \mathbb{R}^{6n_c}$ and contact Jacobians $\mathbf{J}_c : \mathcal{Q} \to \mathbb{R}^{6n_c\times d}$.

Defining the state as $\mathbf{x} = \begin{bmatrix}\mathbf{q}^\top & \dot{\mathbf{q}}^\top\end{bmatrix}^\top$, and the control inputs to optimize over as $\mathbf{u} = \begin{bmatrix}\ddot{\mathbf{q}}_j^\top, & \boldsymbol{\lambda}^\top\end{bmatrix}^\top$, the system dynamics may be rewritten to interpret the joint accelerations $\ddot{\mathbf{q}}_j$ and contact forces $\boldsymbol{\lambda}$, instead of the torques $\boldsymbol{\tau}$, as inputs. The computational benefit of this reparametrization has been shown for reactive whole-body control [17] and offline trajectory optimization [18]. To see this, we write the dynamics in terms of non-actuated base coordinates and fully actuated joint coordinates:

$$\dot{\mathbf{x}} = \begin{bmatrix}\dot{\mathbf{q}}\\ \mathbf{D}_{bb}^{-1}\left(-\mathbf{h}_b - \mathbf{D}_{bj}\ddot{\mathbf{q}}_j + \mathbf{J}_{c,b}^\top\boldsymbol{\lambda}\right)\\ \ddot{\mathbf{q}}_j\end{bmatrix}. \tag{4}$$

The corresponding joint torques may be expressed as:

$$\boldsymbol{\tau} = \mathbf{B}_j^{-1}\left(\mathbf{D}_{bj}^\top\ddot{\mathbf{q}}_b + \mathbf{h}_j + \begin{bmatrix}\mathbf{D}_{jj} & -\mathbf{J}_{c,j}^\top\end{bmatrix}\begin{bmatrix}\ddot{\mathbf{q}}_j\\ \boldsymbol{\lambda}\end{bmatrix}\right). \tag{5}$$

The dynamics in (4) fully encode the challenge of underactuation and encapsulate the core of the floating-base dynamics. Equation (5) plays a secondary role and is only required when formulating torques constraints.

The contact transition maps in (1d) have been set to identity maps for now and will be investigated in future work.

### B. Cost Functions

The cost function is formulated as a nonlinear least square cost around a given state $\boldsymbol{\varepsilon}_x$, input $\boldsymbol{\varepsilon}_u$ and cartesian swing leg $\boldsymbol{\varepsilon}_i$ reference trajectory.

$$l(\mathbf{x}, \mathbf{u}, t) = \frac{1}{2}\boldsymbol{\varepsilon}_x^\top\mathbf{Q}\boldsymbol{\varepsilon}_x + \frac{1}{2}\boldsymbol{\varepsilon}_u^\top\mathbf{R}\boldsymbol{\varepsilon}_u + \frac{1}{2}\sum_i \boldsymbol{\varepsilon}_i^\top\mathbf{W}\boldsymbol{\varepsilon}_i, \tag{6}$$

where $\mathbf{Q}, \mathbf{R}$, and $\mathbf{W}$ are positive definite weighting matrices.

The references are defined heuristically (see Section II-C) or via a walking gait synthesized offline using HZD.

TABLE I: MPC Planning Frequency (10 SQP Iterations)

| Horizon Length [s] | 2.0 | 1.0 | 0.5 | 0.2 |
|---|---|---|---|---|
| MPC Frequency [Hz] | 270 | 480 | 670 | 850 |

### C. Reference Trajectories

*a) HZD Trajectory:* HZD state and input reference trajectories, $\mathbf{x}_{\text{ref}}(t)$ and $\mathbf{u}_{\text{ref}}(t)$, are found offline for the whole-body nonlinear dynamics using the FROST toolbox [19] and stored as Bézier polynomials. This process is completed by fixing a target gait sequence and a forward velocity, and adding various other state and input constraints to a nonlinear trajectory optimization program which ensure the underactuated dynamics of the system display stable periodic behavior. For planar systems, stability can be enforced directly in the optimization program [20], and for general systems it can be verified *a-posteriori* via the Poincaré return map [11].

*b) Heuristic Trajectory:* To evaluate the relative impact of using a gait synthesized offline via HZD in the cost function, we produce a heuristic reference trajectory, using nominal joint configurations and gravity compensating inputs, to be compared against.

### D. Constraints

The following constraints are imposed in problem (1).

1) *Zero force on swing foot*
2) *Zero acceleration on stance foot*
3) *Contact force lies within friction cone*
4) *Torque limits using (5)*

### E. Low-Level Controller

Tthe state and input trajectories generated by MPC are interpolated at a high frequency and converted to a feed-forward control torques, $\boldsymbol{\tau}_{\text{MPC}}$, via (5). Model errors are compensated by adding a proportional-derivative torque, $\boldsymbol{\tau}_{\text{PD}}$, and a friction compensation torque, $\boldsymbol{\tau}_{\text{FC}}$, to the feed-forward torque:

$$\boldsymbol{\tau} = \boldsymbol{\tau}_{\text{MPC}} + \boldsymbol{\tau}_{\text{PD}} + \boldsymbol{\tau}_{\text{FC}}. \tag{7}$$

## III. AMBER Implementation & Results

The AMBER-3M platform is a 5-link planar bipedal robot, which has four open loop torque controlled BLDC motors connected via harmonic drives to the hip and knee joints. All planning, control, and estimation loops were done on separate threads on an offboard Ryzen 9 5950x CPU @ $3.4\,\text{GHz}$. Benchmarks of the maximum obtainable MPC frequency for different horizon lengths can be seen in Table I. To isolate how the system's behavior depends on horizon length, all experiments were conducted with a consistent MPC frequency of $100\,\text{Hz}$.

As can be seen in the supplementary video [21], the proposed MPC formulation is capable of simultaneously stabilizing the underactuated system dynamics and synthesizing valid motion trajectories for a broad range of gait pattern and target velocities both in simulation and on hardware. To evaluate the effect of changing reference signals on the feasibility and robustness of the full control pipeline, a sequence of disturbances of increasing magnitude was applied in simulation to different MPC configurations. The results of these simulations are summarized in Table II.

TABLE II: Maximum disturbance rejection and step adaption range (difference between smallest and largest observed step length). MPC planning frequency clamped at 100 Hz.

| | Disturbance Rejection | | | Step Range |
|---|---|---|---|---|
| Horizon Length | 2 s | 0.5 s | 0.2 s | 2 s |
| Lumped Mass MPC | 2 N | - | - | - |
| MPC + No Terminal | 22 N | - | - | 0.63 m |
| MPC + Heuristic | 22 N | 22 N | - | 0.67 m |
| MPC + HZD | 22 N | 22 N | 20 N | 1.10 m |
| HZD + PD | 30 N | | | 0.14 m |

First, we remark that the results of the Lumped Mass MPC confirm the need for whole-body online planning methods, especially for robots like AMBER-3M which have a non-negligible mass distribution concentrated in the legs.

Next, note that the MPC approach fails quickly for shorter horizon length when no terminal cost is present. When a heuristic terminal component is added, the robustness of the system dramatically increases. Furthermore, when the proposed MPC approach is combined with an HZD-based reference trajectory for running and terminal costs, the horizon length can be shortened to as low as 0.2 seconds, which drastically reduces the computational complexity. Finally, it is important to note that at a disturbance of $22\,\text{N}$ during walking the foot begins to slip, causing all of the MPC based methods to fail. The HZD with PD method exhibits more robustness to foot slipping and is therefore able to endure larger disturbances, as it does not model the disturbances. On the other hand, the MPC methods naturally have a large variability in footstep locations in order to stabilize the system which we believe will be critical for bipedal robots operating on real-world terrain.

The MPC with a heuristic reference trajectory and a horizon length of 1.0 second, and the MPC with an HZD trajectory and a horizon length of 0.5 seconds were then deployed on the AMBER hardware. As seen in Fig. 2, both methods produce forward walking and have a visually distinct gait.

## IV. Conclusion and Outlook

In this work, we proposed a whole-body nonlinear MPC framework that enables online gait optimization using the full rigid body dynamics of a bipedal system. The viability of the presented control structure was shown in simulation and on hardware in a variety of robust dynamic behaviors, including standing, stepping in place, and walking. The addition of a trajectory tracking cost around an offline generated HZD reference enabled similarly robust locomotion at a significantly shorter planning horizon when compared with a heuristic reference or no reference. Motivated by the experimental results and promising reduction in computational complexity, future work will investigate the theoretical properties of using HZD trajectories as terminal components, as well as extensions to 3D walking bipeds.

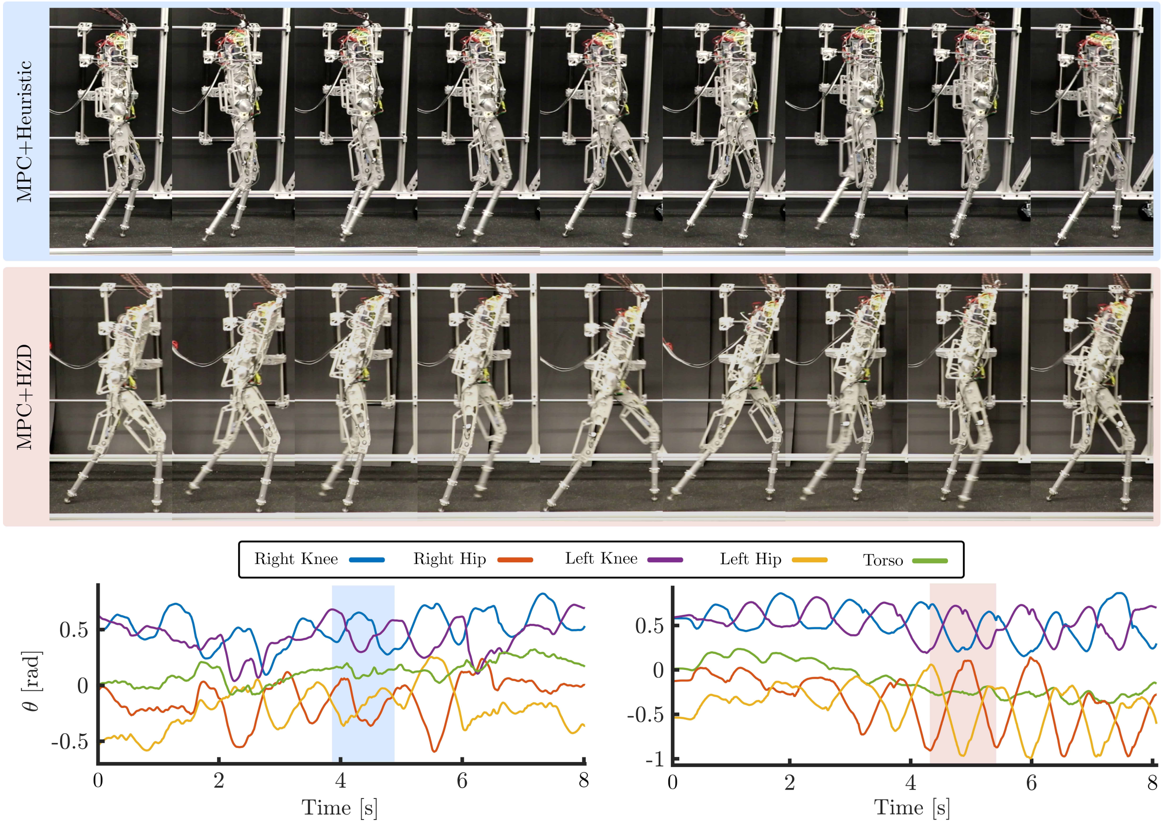


Fig. 2: Gait tiles and joint angle trajectories for forward walking behavior of the whole body MPC at a horizon length of 1 second (top, left), and the whole body MPC+HZD at a horizon length of 0.5 seconds (bottom, right).

## References


[1] M. Vukobratović and B. Borovac, "Zero-moment point—thirty five years of its life," *International journal of humanoid robotics*, vol. 1, no. 01, pp. 157–173, 2004.

[2] S. Kajita, F. Kanehiro, K. Kaneko, K. Yokoi, and H. Hirukawa, "The 3d linear inverted pendulum mode: A simple modeling for a biped walking pattern generation," in *International Conference on Intelligent Robots and Systems (IROS)*, vol. 1. IEEE/RSJ, 2001, pp. 239–246.

[3] T. Koolen, T. De Boer, J. Rebula, A. Goswami, and J. Pratt, "Capturability-based analysis and control of legged locomotion, part 1: Theory and application to three simple gait models," *The international journal of robotics research*, vol. 31, no. 9, pp. 1094–1113, 2012.

[4] C. Mastalli, R. Budhiraja, W. Merkt, G. Saurel, B. Hammoud, M. Naveau, J. Carpentier, L. Righetti, S. Vijayakumar, and N. Mansard, "Crocoddyl: An efficient and versatile framework for multi-contact optimal control," in *International Conference on Robotics and Automation (ICRA)*. IEEE, 2020, pp. 2536–2542.

[5] J.-P. Sleiman, F. Farshidian, M. V. Minniti, and M. Hutter, "A unified mpc framework for whole-body dynamic locomotion and manipulation," *Robotics and Automation Letters*, vol. 6, no. 3, pp. 4688–4695, 2021.

[6] J. Di Carlo, P. M. Wensing, B. Katz, G. Bledt, and S. Kim, "Dynamic locomotion in the mit cheetah 3 through convex model-predictive control," in *International Conference on Intelligent Robots and Systems (IROS)*. IEEE/RSJ, 2018, pp. 1–9.

[7] S. Faraji, S. Pouya, C. G. Atkeson, and A. J. Ijspeert, "Versatile and robust 3d walking with a simulated humanoid robot (atlas): A model predictive control approach," in *International Conference on Robotics and Automation (ICRA)*. IEEE, 2014, pp. 1943–1950.

[8] H. Dai, A. Valenzuela, and R. Tedrake, "Whole-body motion planning with centroidal dynamics and full kinematics," in *International Conference on Humanoid Robots*. IEEE-RAS, 2014, pp. 295–302.

[9] J. Koenemann, A. Del Prete, Y. Tassa, E. Todorov, O. Stasse, M. Bennewitz, and N. Mansard, "Whole-body model-predictive control applied to the hrp-2 humanoid," in *International Conference on Intelligent Robots and Systems*. IEEE/RSJ, 2015, pp. 3346–3351.

[10] F. Farshidian, M. Neunert, A. W. Winkler, G. Rey, and J. Buchli, "An efficient optimal planning and control framework for quadrupedal locomotion," in *International Conference on Robotics and Automation (ICRA)*. IEEE, 2017, pp. 93–100.

[11] E. R. Westervelt, J. W. Grizzle, C. Chevallereau, J. H. Choi, and B. Morris, *Feedback Control of Dynamic Bipedal Robot Locomotion*. Taylor & Francis/CRC Press, 2007.

[12] E. Ambrose, W.-L. Ma, C. Hubicki, and A. D. Ames, "Toward benchmarking locomotion economy across design configurations on the modular robot: Amber-3m," in *Conference on Control Technology and Applications (CCTA)*. IEEE, 2017, pp. 1270–1276.

[13] M. Diehl, H. G. Bock, H. Diedam, and P.-B. Wieber, "Fast direct multiple shooting algorithms for optimal robot control," in *Fast motions in biomechanics and robotics*. Springer, 2006, pp. 65–93.

[14] "OCS2: An open source library for optimal control of switched systems," [Online]. Available: https://github.com/leggedrobotics/ocs2.

[15] J. Carpentier, G. Saurel, G. Buondonno, J. Mirabel, F. Lamiraux, O. Stasse, and N. Mansard, "The pinocchio c++ library: A fast and flexible implementation of rigid body dynamics algorithms and their analytical derivatives," in *International Symposium on System Integration (SII)*. IEEE/SICE, 2019, pp. 614–619.

[16] B. M. Bell, "Cppad: a package for c++ algorithmic differentiation," *Computational Infrastructure for Operations Research*, vol. 57, no. 10, 2012.

[17] C. D. Bellicoso, F. Jenelten, P. Fankhauser, C. Gehring, J. Hwangbo, and M. Hutter, "Dynamic locomotion and whole-body control for quadrupedal robots," in *International Conference on Intelligent Robots and Systems (IROS)*. IEEE/RSJ, 2017, pp. 3359–3365.

[18] H. Ferrolho, V. Ivan, W. Merkt, I. Havoutis, and S. Vijayakumar, "Inverse dynamics vs. forward dynamics in direct transcription formulations for trajectory optimization," in *International Conference on Robotics and Automation (ICRA)*. IEEE, 2021, pp. 12 752–12 758.

[19] A. Hereid and A. D. Ames, "Frost∗: Fast robot optimization and simulation toolkit," in *International Conference on Intelligent Robots and Systems (IROS)*. IEEE/RSJ, 2017, pp. 719–726.

[20] A. D. Ames, "Human-inspired control of bipedal walking robots," *Transactions on Automatic Control*, vol. 59, no. 5, pp. 1115–1130, 2014.

[21] "Video of the experimental results." https://youtu.be/3g8ZNsCWdOA.